symmetry

MDPI

*Article*

# Dynamic Responses of Train-Symmetry-Bridge System Considering Concrete Creep and the Creep-Induced Track Irregularity

**Wenfeng Li [1], Hongkai Ma [1], Minglong Wei [1,2,*], Ping Xiang [1], Fang Tang [3], Binwei Gao [4] and Qishi Zhou [1]**

1 School of Civil Engineering, Central South University, Changsha 410075, China; mahongkai@csu.edu.cn (H.M.); pxiang@csu.edu.cn (P.X.)
2 Hefei Bangcheng Hetai Real Estate Co., Ltd., Hefei 230000, China
3 Changsha Health Vocational College, Changsha 410075, China
4 School of Architecture and Civil Engineering, Xiamen University, Xiamen 361005, China
* Correspondence: 214811103@csu.edu.cn

**Abstract:** This work considers the influence of concrete creep on track irregularities and establishes the dynamic motion equation of the train-track-bridge coupling system. The track irregularity is obtained by superposition of the initial geometric irregularity and additional geometric irregularity of the steel rail caused by creep. When high-speed railway trains pass through bridges; the vertical acceleration and vertical displacement of continuous beam bridges are related to the train's operating speed, and the influence of creep camber is relatively small. At the same time, considering the randomness of track irregularities, the dynamic responses of the train track bridge coupling system under the action of random track irregularities are analyzed, and the dynamic responses of trains at different operating speeds are obtained. The deterministic and uncertain dynamic responses of the train track bridge system were compared and analyzed to verify the accuracy of the Karhunen Loéve expansion (KLE)-Point estimate method (PEM) calculation results. The results indicate that the random characteristics of track irregularities have a significant impact on train dynamic response. Based on the random system vibration analysis and considering the safety and comfort indicators of high-speed railway trains, the creep deformation limit of a continuous beam bridge with a length of 48 m + 80 m + 48 m is obtained to be 19 mm. This is the first time that the dynamic responses of train-symmetry-bridge system are calculated by considering concrete creep and the creep-induced track irregularity, which has certain significance for understanding the dynamics of train -bridge system. In addition, the proposed creep threshold is also of great significance to ensure the safety of traveling.

**Keywords:** concrete creep; track irregularity; train-track-bridge system; vibration analysis

check for updates

**Citation:** Li, W.; Ma, H.; Wei, M.; Xiang, P.; Tang, F.; Gao, B.; Zhou, Q. Dynamic Responses of Train-Symmetry-Bridge System Considering Concrete Creep and the Creep-Induced Track Irregularity. *Symmetry* **2023**, *15*, 1846. https://doi.org/10.3390/sym15101846

Academic Editor: Sergei Alexandrov

Received: 23 July 2023
Revised: 10 September 2023
Accepted: 18 September 2023
Published: 29 September 2023



## 1. Introduction

Nowadays, China's high-speed railway technology is at the top level globally, and efforts are being made to build high-speed railways domestically [1]. Prestressing tendons distributed in the box volume of a simply supported girder bridge will be prestressed at various locations in the girder. The prestressing tendons cause the pre-compressive stress to vary regularly along the height of the girder, so that the girder will deform vertically upward at various locations with this action [2,3]. Bridges account for a large proportion in high-speed railway lines, and the structure of bridges is mainly divided into continuous beam bridges and simply supported beam bridges. Compared to simply supported beams, the advantages of continuous beam bridges are their large span, strong integrity, low track unevenness, and small beam end deformation angle [4]. Therefore, continuous beam bridges have great competitive advantages in the construction process of high-speed railway large-span bridges. High speed railway trains operate at high speeds and require high levels of safety and comfort, thus requiring high levels of track smoothness [5]. Especially for continuous beam bridge structures, which use large volume concrete, the shrinkage and creep of prestressed concrete can cause arch deformation of the bridge, which will affect the smoothness of the bridge deck [6].

If the bridge deformation and disease due to creep, settlement and girder misalignment, etc., will have a serious impact on the high-speed railroad train operation, driving safety [7]. The effects of creep can lead to a vertical upset in which the track changes periodically and regularly, and the effects of creep can continue to develop and exacerbate the vertical upset [8,9]. At the same time, in addition to creep, tracks and bridges are also affected by construction technology, pavement processing, temperature and humidity, so track unevenness is random [10].

In order to ensure that the smoothness of the track meets the requirements for designing high-speed railway train operation, it is necessary to study the safety and comfort of high-speed railway trains caused by track irregularities caused by bridge creep deformation after track laying [11]. At the same time, track irregularity has random characteristics, requiring random vibration analysis of the high-speed railway train track bridge coupling system [12,13].

In order to ensure that the smoothness of the track meets the operational requirements of high-speed trains, it is necessary to study the impact of track irregularities caused by bridge creep deformation on the safety of high-speed railway trains. The train track bridge coupling system is a complex system that involves the intersection of multiple disciplines and numerous random factors, such as the randomness of track irregularities, bridge parameters, and earthquakes [14,15]. However, in previous studies and specifications, the impact of track irregularity randomness on high-speed railway train operation was not considered, which led to the lack of authenticity of the vehicle bridge coupling system studied [16,17]. The most common calculation method for random vibration is the Monte Carlo method, but its disadvantage is that it requires a large number of calculation samples, which restricts its practical application. The running safety of the train track bridge coupling system were also investigated, but the initial unevenness of the track in this part is not random [18]. In practical situations, the initial unevenness of the track has random characteristics, and the randomness of the track will have random characteristics on the dynamic response of the vehicle body [19,20]. Therefore, it is necessary to considering the randomness of track irregularity, the vibration of the train track bridge system can more accurately and truly reflect the actual motion state of the train [5].

In this work, the continuous beam bridges are considered as the research object to study the creep deformation of concrete materials in prestressed concrete continuous beam bridges, as well as the influence of random factors on the safety of high-speed railway trains. This is the first time that the dynamic responses of train-symmetry-bridge system are calculated by considering concrete creep and the creep-induced track irregularity. This paper first introduces the theory of Karhunen Loéve expansion (KLE) [21] method and point estimation method. The KLE method is used to express the track irregularity and input it into the train track bridge coupling system, and then the point estimation method (PEM) is used to calculate the random response results [22], which is called KLE-PEM method for short. Taking the 48 m + 80 m + 48 m continuous beam bridge and CRH2 train as the mock object, the random dynamic response of the train is analyzed through numerical simulation, and the running safety and comfort of the train are analyzed.

## 2. Random Vibration Theory Based on KLE-PEM

The randomness of orbital unevenness is represented by the KLE method. Among the many methods for representing random processes, the KLE method is undoubtedly an effective method, which has the advantage of obtaining expressions with sufficient probability information with fewer random variables. According to the literature [1], the basic expression form of the KL expansion is

$$r(x,\theta) = \bar{r}(x,\theta) + \sum_{n=1}^{M} \sqrt{\lambda_n}\xi_n(\theta)\varphi_n(x) \tag{1}$$

where, $r(x,\theta)$ is represented as a Gaussian random process and $\xi_n(\theta)$ is represented as a set of unrelated random variables that follow a standard normal distribution. $\lambda_n$ and $\varphi_n(x)$ are represented as eigenvalues and eigenfunctions, respectively, and the value of M determines the precision of the random field representation.

Point estimation will be used to calculate random responses. According to the theory of point estimation, the expectation of the stochastic system Y and variance can be calculated using the following equation

$$E[Y] \cong \sum_{i=1}^{n} E[g_i(X_i)] - (n-1)g(c), \tag{2}$$

$$M_{z2} = D[Y] \cong \sum_{i=1}^{n} \left\{ [g_i(X_i) - \mu]^2 \right\} - (n-1)[g(c) - \mu]^2, \tag{3}$$

with $\mu = E[Y]$, $M_{z2}$ represents the variance of $Y$.

According to $E[g_i(X_i)]$ and $E\left[[g_i(X_i) - \mu]^2\right]$ in Formulas (2) and (3), the following equation can be derived:

$$[g_i(X_i)] = \sum_{l=1}^{r} \frac{\omega_{GH,l}}{\sqrt{\pi}} g_i\left(\sqrt{2}x_{GH,l}\right), \tag{4}$$

$$E\left[(g_i(X_i) - \mu)^2\right] = \sum_{l=1}^{r} \frac{\omega_{GH,l}}{\sqrt{\pi}} \left[g_i\left(\sqrt{2}x_{GH,l}\right) - \mu\right]^2, \tag{5}$$

where $r$ is the estimated number of points for the Gaussian-Hermite integral, while $x_{GH,l}$ and $\omega_{GH,l}$ are respectively Gaussian-Hermite's abscissa and weights of Hermite, the specific values of the list integration points, are shown in Table 1.

**Table 1.** Point Gaussian Hermite integration abscissa and weight coefficients [23].

| Point | 1 | 2 | 3 |
|---|---|---|---|
| $x_{GH,l}$ | −1.22474 | 0 | 1.22474 |
| $\omega_{GH,l}$ | 0.29541 | 1.18146 | 0.29541 |

## 3. Expression of Track Irregularity Based on KLE

Track irregularity samples are obtained by actual measurement of railway tracks or power spectral density conversion [24]. Using a large number of spatial samples, the eigenfunctions and eigenvalues represented by the KL expansion with uneven orbits can be derived. Firstly we suppose that the orbital unevenness $\widetilde{z}R(x,\theta)$ is a Gaussian random process that can be expressed by KLE as:

$$z(x,\theta) = \bar{z}(x) + \sum_{k=1}^{m} \sqrt{\lambda_k}\xi_k\varphi_k(x,\theta), \tag{6}$$

With $\xi_k$ represents a set of random variables that are independently distributed from each other. Typically, Track irregularity is a zero mean stochastic process. However, since the deformation of the rail caused by bridge creep is considered in this article, the track in this article, unevenness is a random process with zero non-mean, i.e., $z(x) = z^{creep}(x)$ is the deformation of the rail caused by the creep of the bridge.

After obtaining the track unevenness sample, the dynamic response of the train-track-bridge coupling system can be obtained by calculating the unevenness amplitude in the transformation model and acting on the wheel-rail force of the train-track-bridge coupling system as an external excitation. When the point estimation method is used for random response calculations, the zero point can be used as a reference point. When the response of the random system is calculated by the point estimation method, the k-th random variable corresponding to the l-th Gaussian point can be expressed as:

$$\widetilde{z}_{k,l} = z^{creep}(x) + \sqrt{2}x_{GH,l}\sqrt{\lambda_k}\varphi_k(x), \tag{7}$$

where, $z^{creep}(x)$ is the deformation of the track, $\lambda_k$ and $\varphi_k$ are, respectively the eigenvalues and eigenfunctions (normalized) of the KLE

Taking the displacement response of a certain time t of the bridge as an example, the corresponding response $R(k,l,t)$ of the system can be obtained by calculating the orbital uneven sample corresponding to the Gaussian point of each random variable as the orbital uneven sample of the system Arrive. The corresponding response for a zero-uneven sample is $R_0(t)$. The expectation and variance of the response can be achieved by putting all the $R(k,l,t)$ and $R_0$ into Equations (2) and (3):

$$Mean\cdot(t) \approx \sum_{k=1}^{m}\sum_{l=1}^{r}\frac{\omega_{GH,l}}{\sqrt{\pi}}R(k,l,t) - (m-1)R_0(t), \tag{8}$$

$$Var\cdot(t) = \sum_{k=1}^{m}\sum_{l=1}^{r}\frac{\omega_{GH,l}}{\sqrt{\pi}}[R(k,l,t) - Mean\cdot(t)]^2 - (m-1)[R_0 - Mean\cdot(t)]^2 \tag{9}$$

Except for the non-zero Gaussian point of the k-th random variable, all other samples of orbital irregularities are zero amplitude irregularities, i.e., $R(k,(r+1)/2,t) = R_0(t)$. The standard deviation of the response can be obtained by the following formula:

$$Std.D(t) = \sqrt{Var\cdot(t)}, \tag{10}$$

where, $Std.D(t)$ is the standard deviation of the response.

## 4. Dynamic Response Analysis of Uncertain Systems

### *4.1. Validation of KLE-PEM Method*

Multi-rigid-body dynamics is used to establish the vehicle model, the track plate, base plate and bridge structure are established by beam and plate unit, and the upper structure is linked to the lower structure through the wheel-rail coupling relationship, which constitutes the train-rail-bridge system [25]. The model used in this paper is the same as that in the literature, in which the field test results are compared with the numerical simulation results, and it is found that the two are in good agreement, which verifies the correctness of the model. In summary, it shows that the model and numerical framework established in this paper are reliable.

In this section, 10,000 track irregularity samples are obtained by trigonometric series method to simulate the train track bridge coupling system with Monte Carlo method, and verify the accuracy, adaptability and superiority of KLE-PEM method. The parameters and layout of the bridge structure have been explained in Ref. [26]. The train adopts the CRH2 model of the Chinese high-speed multiple unit train, consisting of 2 multiple units and 6 trailers, with a total of 8 car bodies. The parameters of the train are shown in Table 2, and the main parameters of the bridge are shown in Table 2. The running speed of the train is 300 km/h, and the length of the approach bridge on both sides of the bridge is 100 m. The purpose is to eliminate the rail boundary effect in the roadbed section, and it is assumed that the approach bridge section is rigid. The parameters of track irregularity consider their randomness, while other bridge parameters do not consider their randomness. Figure 1 depicts the time history response of the vertical acceleration in the span of a continuous beam bridge, with its horizontal coordinates representing the operating time of the first wheelset passing through the left side of the bridge.

**Table 2.** Main Parameters of Bridges.

| Parameters | Units | Numerical Value |
|---|---|---|
| Elastic modulus of bridge | $N/m^2$ | $3.45 \times 10^{10}$ |
| Elastic modulus of track plate | $N/m^2$ | $2.06 \times 10^{11}$ |
| Cross section mass moment of inertia | $m^4$ | 12.744 |
| Poisson's ratio | — | 0.2 |
| Mass per unit length | kg/m | $2.972 \times 10^4$ |
| Beam unit length | m | 0.64 |
| Damping ratio | — | 0.05 |
| First natural frequency | Hz | 2.25 |
| Second natural frequency | Hz | 4.81 |
| Third natural frequency | Hz | 5.65 |
| Fourth natural frequency | Hz | 5.93 |

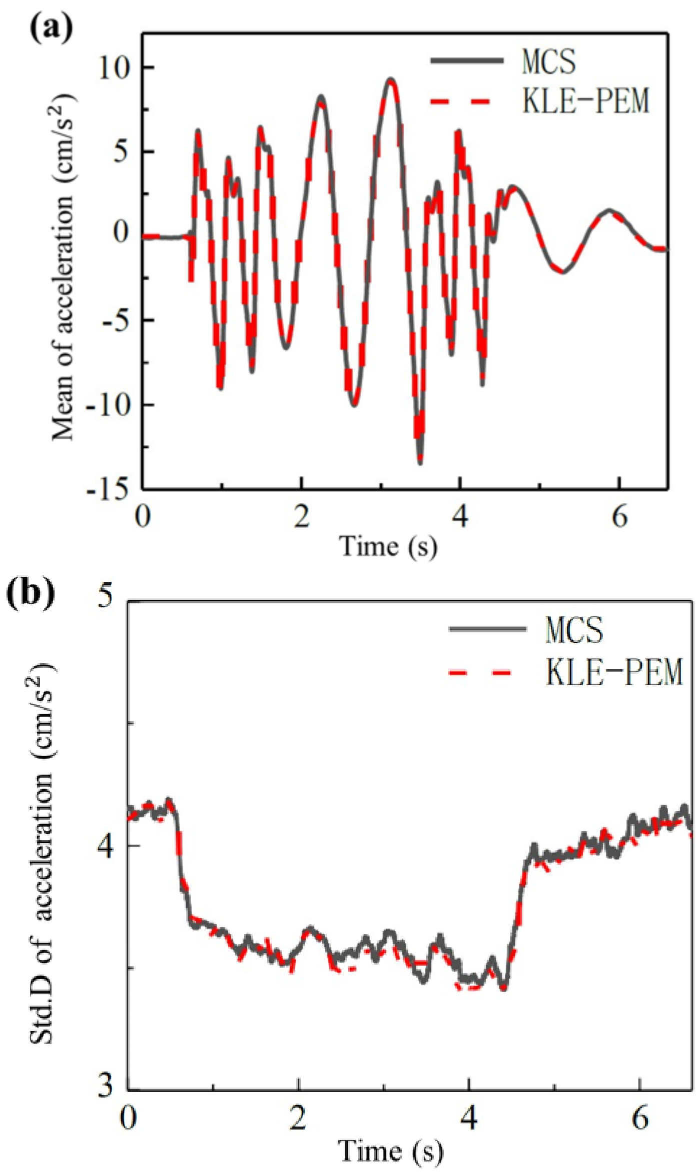


**Figure 1.** Comparison of Mid span Acceleration of Continuous Beam Bridges.

From Figure 1a,b, it can be observed that the mean and standard deviation curves of bridge acceleration obtained by the KLE-PEM method tend to be consistent with the curves simulated by the Monte Carlo method. The error in the mean and standard deviation of the responses calculated by the two calculation methods is very small, and this error is objective and within the permissible limits of the calculation methods. Generally speaking, this shows that the stochastic response of the bridge calculated using the KLE-PEM method has high accuracy and computational efficiency.

### *4.2. Comparison of Train Certainty Analysis and Uncertainty Analysis*

This section will compare the deterministic analysis and uncertainty analysis of train dynamic response. The bridge models selected for the deterministic and uncertainty analysis of vehicle dynamic response are both continuous beam bridges and simply supported beam bridges, with a total of 7 spans and a length of 304 m. The train adopts the CRH2 model of China High Speed Multiple Unit, as shown in Figure 2, and the bridge and train parameters are in Ref. [26]. The main difference between deterministic analysis and uncertainty analysis of train dynamic response lies in the initial unevenness of the track. The track irregularity in deterministic analysis is obtained by selecting 10 random tracks with initial irregularity and additional irregularity superimposed to obtain track irregularity; The uncertainty analysis of track irregularity is achieved by obtaining the initial random irregularity of the track using the KLE-PEM method, and then adding it to the additional irregularity to obtain the track irregularity.

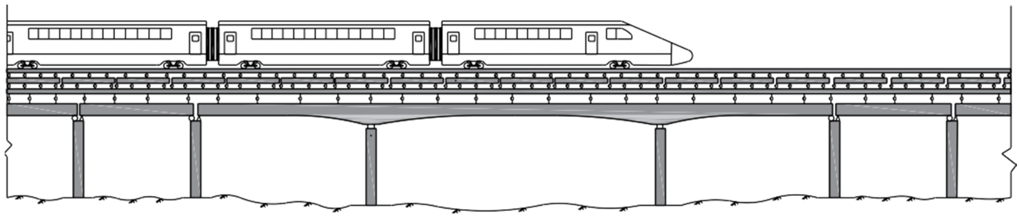

**Figure 2.** China high speed train model.

The KLE-PEM method can be used to obtain the mean and standard deviation of the train track bridge coupling system. According to the probability distribution function of normal distribution, the probability of value distribution within the range of (mean value − 3 times standard deviation, mean value + 3 times standard deviation) is 99.73%, which is used to determine the extreme value response of the train. Therefore, the dynamic response of the vehicle body is determined by selecting the maximum absolute value of the mean plus or minus three times the standard deviation.

The calculation results are shown in Figure 3, which contains the values of the vertical acceleration of the front and rear bogie bodies that are indeed analyzed qualitatively and stochastically. From Figure 3a, it can be seen that the vertical acceleration of the vehicle body above the front bogie has the same trend in both deterministic and uncertainty analysis. However, the maximum acceleration for uncertainty analysis is 0.41 m/s$^2$, while the maximum acceleration for deterministic analysis is 0.29 m/s$^2$, which is 41.4% higher. From Figure 3b, it can be observed that there is a difference in the trend of qualitative analysis and uncertainty analysis for the acceleration of the vehicle body above the bogie. The maximum vertical acceleration for uncertainty analysis is 0.61 m/s$^2$, while the maximum acceleration for certainty analysis is 0.48 m/s$^2$, which is 27.1% higher.

In summary, the dynamic response of the train does differ significantly between the qualitative and uncertainty analyses, and the response obtained from the stochastic analysis is significantly larger than that obtained under determinism. Rather than assuming fixed values, stochastic analysis uses probability distributions to model uncertainty. As a result, the response in a stochastic analysis will vary from simulation to simulation, leading to a wider range of possible outcomes. Therefore, considering the random vibration analysis of the train track bridge coupling system can more accurately reflect the actual operation of the train, and the results can provide theoretical suggestions for the design and construction of high-speed railways.

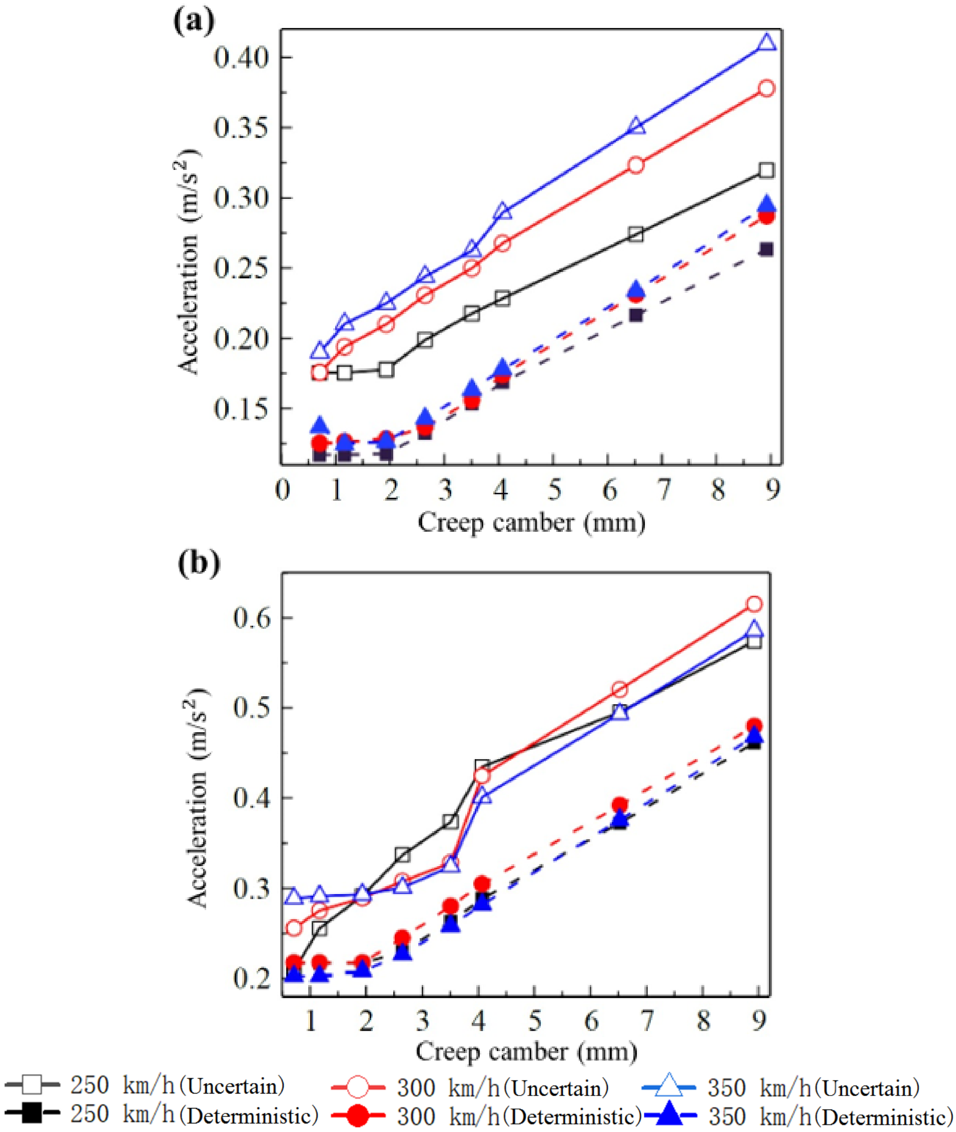


**Figure 3.** Comparison of Deterministic and Uncertain Analysis of Vehicle Acceleration: (**a**) Position above the front bogie (**b**) Position above the rear bogie.

### 4.3. *Response of Trains*

The different operating speeds of trains will have different dynamic responses to the train track bridge coupling system. When a train passes through a bridge, it will vibrate the bridge, and resonance phenomenon will occur at a specific operating speed. This will affect the service life of the bridge, as well as the safety and comfort of train operation. This section uses three train operating speeds of 250 km/h, 300 km/h, and 350 km/h to study the random dynamic response of the train track bridge coupling system at different speeds. An analysis was conducted on a 7-span simply supported beam bridge and continuous beam bridge system. The train adopts the CRH2 model of the Chinese high-speed multiple unit train, consisting of 2 high-speed trains and 6 trailers. The parameters of the bridge and train are explained in Ref. [26].

The external excitation of the train track bridge coupling system is generated through track irregularity, which in this section is the superposition of the initial irregularity of the steel rail and the additional irregularity caused by bridge deformation. The initial irregularity of the steel rail is considered for its randomness, and the initial random irregularity of the track is obtained through the KLE-PEM method. The additional irregularity is selected from the residual deformation caused by the creep of the bridge from six months to ten years. A total of 12 additional irregularities are selected, and then stacked to obtain the track irregularity.

Figure 4 respectively describe the acceleration response of the vehicle body above the front and rear bogies at different train operating speeds. From Figure 4, it can be observed that the acceleration of the vehicle body above the front and rear bogies of the train increases with the increase of creep camber at the determined operating speed. In Figure 4a, the acceleration of the vehicle above the front bogie increases with the increase of operating speed. When the train operates at a speed of 350 km/h and the creep camber reaches 22.5 mm, the vertical acceleration of the vehicle reaches a maximum of 0.82 m/s$^2$. In Figure 4b, the acceleration of the vehicle above the rear bogie increases with the increase of creep camber, reaching a speed of 300 km/s and a camber of 22.5 mm, the maximum vertical acceleration of the vehicle body reaches 1.37 m/s$^2$. According to the Chinese standard for operational comfort, it is recommended that the vertical acceleration of the vehicle body should not exceed the limit of 0.13 g (=1.275 m/s$^2$). From Figure 4b, it can be seen that the train running speed is 250 km/h, and the corresponding creep camber amplitude for an acceleration of 1.275 m/s$^2$ is 19 mm. Overall, stochastic analysis can be used to effectively calculate the relationship between creep and response, which is important for ensuring traffic safety.

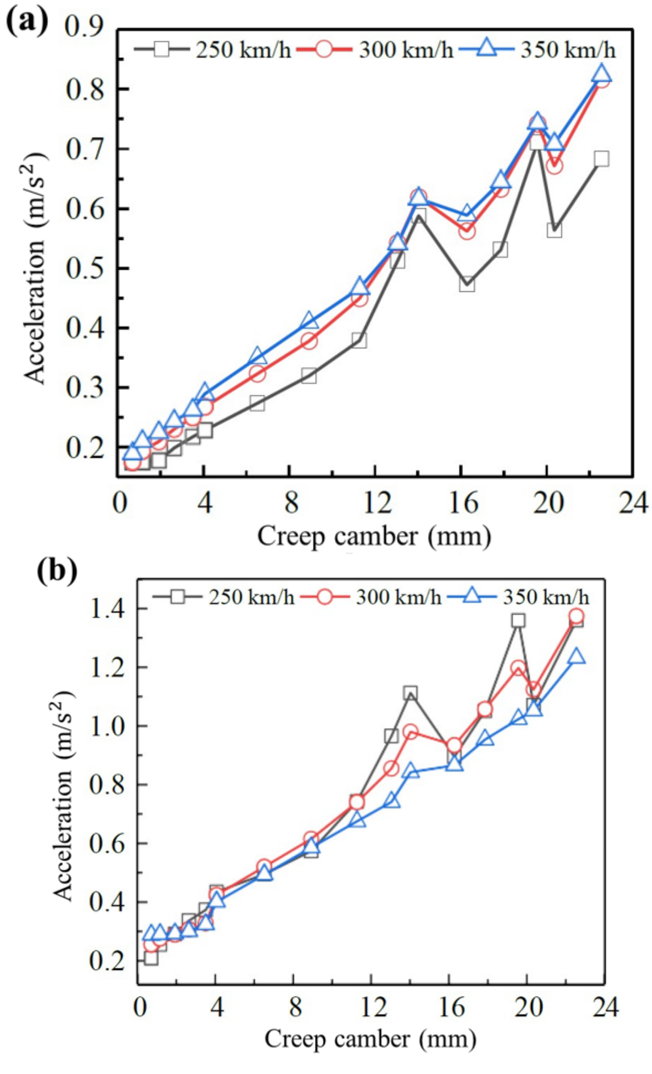


**Figure 4.** Vertical acceleration of vehicle: (**a**) Position above the front bogie (**b**) Position above the rear bogie.

Figure 5 describe the wheel load reduction rate of the CRH2 model train, and it can be seen from the figure that the wheel load reduction rate increases with the increase of roughness amplitude. And at a train speed of 250 km/h and a creep camber of 22.5 mm, the maximum wheel load reduction rate is 0.63. According to the standard, the wheel load reduction rate is less than the standard limit value of 0.6. Based on Figure 5, it can be seen that the vehicle speed is 250 km/h, the creep camber is 21 mm, and the wheel load reduction rate reaches 0.6.

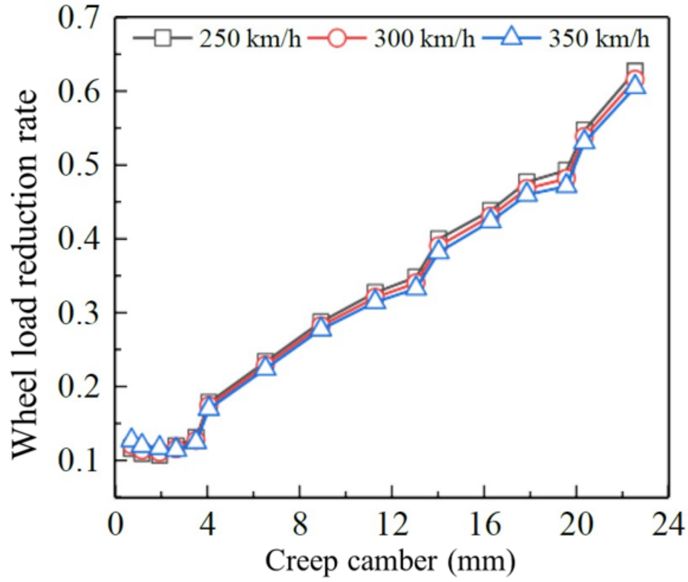


**Figure 5.** Wheel load reduction rate.

Table 3 shows the limit values of camber on continuous beam bridges under different operating speeds of high-speed railway trains, taking into account the random characteristics of track irregularities. Taking into account the safety and comfort indicators of high-speed railway trains, combined with Table 3, it can be concluded that the creep camber limit of continuous beam bridges is 19 mm. Based on the random characteristics of track irregularity, when high-speed railway trains operate on a continuous beam bridge of 48 m + 80 m + 48 m, considering the safety and comfort indicators of the train, a limit value of 19 mm is given for the creep camber of the continuous beam bridge. If this limit is exceeded, it may have a negative impact on travel safety and passenger comfort.

**Table 3.** Camber limit on continuous beam bridges.

| Parameter | Speed (km/h) | | |
|---|---|---|---|
| | **250** | **300** | **350** |
| Safety indicators | 21.1 mm | 21.3 mm | 21.5 mm |
| Comfort indicators | 19.0 mm | 21.6 mm | 21.8 mm |

## 5. Conclusions

This chapter analyzes the dynamic response of the train track bridge coupling system under random track irregularities. A train, bridge, and track model was established using finite element method. Considering the randomness of track irregularity, the KLE method is used to represent the stochastic process of initial track irregularity, and then the track irregularity is obtained by superposition with the additional track irregularity. The random response, including mean value and standard deviation, is calculated by the point estimation method. Verify the calculated results with the Monte Carlo simulation results through numerical simulation, and study the dynamic response of different train operating speeds. The main conclusions are as follows:

(1) By comparing with the Monte Carlo method, the accuracy of the KLE-PEM method was verified, and the KLE-PEM method has higher computational efficiency.
(2) There is a significant difference between the deterministic dynamic response analysis and the uncertain dynamic response analysis of the train track bridge system. The uncertainty dynamic analysis of the train track bridge system can more accurately and effectively reflect the actual situation of the train during operation.
(3) The vertical acceleration of the vehicle body above the front bogie of the train increases with the increase of train operating speed; The vertical acceleration and wheel load reduction rate of the vehicle body above the front and rear bogies increase with the increase of the upper creep camber; Based on the safety and comfort indicators of train operation, the creep upper arch limit of a 48 m + 80 m + 48 m continuous beam bridge is given as 19 mm.

Overall, the study of the response of vehicles under creep and random track irregularities, and the derivation of a limit value of creep late arching under a probabilistic angle, are of some guidance significance for the design of continuous girder bridges of high-speed railroads from the front-end of the design to the back-end of the operation.

In this paper, based on the acceleration of the vehicle body and the wheel weight reduction rate, a threshold value of the creep probability is proposed to ensure the safety and comfort of the vehicle body operation, and it is analyzed for different speeds and different deformation conditions of the upper supply. However, this paper does not propose effective solution measures and further analysis for the creeping upper arch situation. After considering the randomness of creep and track irregularity, how to better control the continuous girder bridge from the source is a problem that the authors need to continue to study.

**Author Contributions:** Conceptualization, Methodology and Writing, W.L. and M.W.; Software and formal analysis, W.L.; Validation, M.W.; Resources and Supervision, P.X. and Q.Z.; Visualization, F.T. and B.G.; Review and Editing, H.M.; Funding acquisition, P.X. All authors have read and agreed to the published version of the manuscript.

**Funding:** This research work was financially supported by the Hunan Natural Science Foundation Science and Education Joint Fund Project 2022JJ60109, Hunan Science Fund for Distinguished Young Scholars (2021JJ10061) and Central South University Research Project Nos. 202045006 and 502390001.

**Data Availability Statement:** Some or all data, models, or code that support the findings of this study are available from the corresponding author upon reasonable request.

**Conflicts of Interest:** The authors declare no conflict of interest. The authors don't have any relevant financial or non-financial competing interests.

## References

1. Jiang, L.Z.; Liu, X.; Xiang, P.; Zhou, W.B. Train-bridge system dynamics analysis with uncertain parameters based on new point estimate method. *Eng. Struct.* **2019**, *199*, 109454. [CrossRef]
2. Trong-Phuoc, H.; Hwang, C.-L.; Limongan, A.H. The long-term creep and shrinkage behaviors of green concrete designed for bridge girder using a densified mixture design algorithm. *Cem. Concr. Compos.* **2018**, *87*, 79–88.
3. Au, F.T.K.; Si, X.T. Accurate time-dependent analysis of concrete bridges considering concrete creep, concrete shrinkage and cable relaxation. *Eng. Struct.* **2011**, *33*, 118–126. [CrossRef]
4. Xiang, P.; Huang, W.; Jiang, L.Z.; Lu, D.G.; Liu, X.; Zhang, Q. Investigations on the influence of prestressed concrete creep on train-track-bridge system. *Constr. Build. Mater.* **2021**, *293*, 123504. [CrossRef]
5. Zhao, H.; Wei, B.; Jiang, L.; Xiang, P. Seismic running safety assessment for stochastic vibration of train–bridge coupled system. *Arch. Civ. Mech. Eng.* **2022**, *22*, 180. [CrossRef]
6. Jiang, L.Z.; Liu, C.; Peng, L.X.; Yan, J.W.; Xiang, P. Dynamic Analysis of Multi-layer Beam Structure of Rail Track System under a Moving Load Based on Mode Decomposition. *J. Vib. Eng. Technol.* **2021**, *9*, 1463–1481. [CrossRef]
7. Nakov, D.; Markovski, G.; Arangjelovski, T.; Mark, P. Experimental and Analytical Analysis of Creep of Steel Fibre Reinforced Concrete. *Period. Polytech.-Civ. Eng.* **2018**, *62*, 226–231. [CrossRef]
8. Chen, Z.; Zhai, W.; Cai, C.; Sun, Y. Safety threshold of high-speed railway pier settlement based on train-track-bridge dynamic interaction. *Sci. China-Technol. Sci.* **2015**, *58*, 202–210. [CrossRef]

9. Rahmanzadeh, S.; Tariverdilo, S. Evaluating Applicability of ASTM C 928 Approach in Assessing Adequacy of Patch Repair of Bridge Piers. *Int. J. Eng.* **2020**, *33*, 2455–2463.
10. Xiong, Z.; Chen, J.; Liu, C.; Li, J.; Li, W. Bridge's Overall Structural Scheme Analysis in High Seismic Risk Permafrost Regions. *Civ. Eng. J.* **2022**, *8*, 1316–1327. [CrossRef]
11. Chan, Y.W.S.; Wang, H.P.; Xiang, P. Optical Fiber Sensors for Monitoring Railway Infrastructures: A Review towards Smart Concept. *Symmetry* **2021**, *13*, 2251. [CrossRef]
12. Wang, X.; Luo, F.; Ye, A. A holistic framework for seismic analysis of extended pile-shaft-supported bridges against different extents of liquefaction and lateral spreading. *Soil Dyn. Earthq. Eng.* **2023**, *170*, 107914. [CrossRef]
13. Wang, X.; Ji, B.; Ye, A. Seismic Behavior of Pile-Group-Supported Bridges in Liquefiable Soils with Crusts Subjected to Potential Scour: Insights from Shake-Table Tests. *J. Geotech. Geoenviron. Eng.* **2020**, *146*, 04020030. [CrossRef]
14. Wang, X.W.; Ye, A.J.; Ji, B.H. Fragility-based sensitivity analysis on the seismic performance of pile-group-supported bridges in liquefiable ground undergoing scour potentials. *Eng. Struct.* **2019**, *198*, 109427. [CrossRef]
15. Wang, X.W.; Ye, A.J.; Shang, Y.; Zhou, L.X. Shake-table investigation of scoured RC pile-group-supported bridges in liquefiable and nonliquefiable soils. *Earthq. Eng. Struct. Dyn.* **2019**, *48*, 1217–1237. [CrossRef]
16. Wang, X.; Ye, A.; Shafieezadeh, A.; Padgett, J.E. Fractional order optimal intensity measures for probabilistic seismic demand modeling of extended pile-shaft-supported bridges in liquefiable and laterally spreading ground. *Soil Dyn. Earthq. Eng.* **2019**, *120*, 301–315. [CrossRef]
17. Wang, X.; Shafieezadeh, A.; Ye, A. Optimal EDPs for Post-Earthquake Damage Assessment of Extended Pile-Shaft-Supported Bridges Subjected to Transverse Spreading. *Earthq. Spectra* **2019**, *35*, 1367–1396. [CrossRef]
18. Xia, Q.; Xiang, P.; Jiang, L.Z.; Yan, J.W.; Peng, L.X. Bending and free vibration and analysis of laminated plates on Winkler foundations based on meshless layerwise theory. *Mech. Adv. Mater. Struct.* **2022**, *29*, 6168–6187. [CrossRef]
19. Yang, D.; Chen, H.; Meng, Z.; Chen, G. Random Vibration and Dynamic Reliability Analyses for Nonlinear MDOF Systems under Additive Excitations via DPIM. *J. Eng. Mech.* **2021**, *147*, 04021117. [CrossRef]
20. Huo, H.; Zhou, Z.; Chen, G.H.; Yang, D.X. Exact benchmark solutions of random vibration responses for thin-walled orthotropic cylindrical shells. *Int. J. Mech. Sci.* **2021**, *207*, 106644. [CrossRef]
21. Liu, X.; Jiang, L.Z.; Xiang, P.; Zhou, W.B.; Lai, Z.P.; Feng, Y.L. Stochastic finite element method based on point estimate and Karhunen-Loeve expansion. *Arch. Appl. Mech.* **2021**, *91*, 1257–1271. [CrossRef]
22. Chen, G.; Zhou, J.; Yang, D. Benchmark solutions of stationary random vibration for rectangular thin plate based on discrete analytical method. *Probabilistic Eng. Mech.* **2017**, *50*, 17–24. [CrossRef]
23. Liu, X.; Xiang, P.; Jiang, L.; Lai, Z.; Zhou, T.; Chen, Y. Stochastic Analysis of Train-Bridge System Using the Karhunen-Loeve Expansion and the Point Estimate Method. *Int. J. Struct. Stab. Dyn.* **2020**, *20*, 2050025. [CrossRef]
24. Zhao, H.; Wei, B.; Jiang, L.; Xiang, P.; Zhang, X.; Ma, H.; Xu, S.; Wang, L.; Wu, H.; Xie, X. A velocity-related running safety assessment index in seismic design for railway bridge. *Mech. Syst. Signal Process.* **2023**, *198*, 110305. [CrossRef]
25. Xiang, P.; Ma, H.; Zhao, H.; Jiang, L.; Xu, S.; Liu, X. Safety analysis of train-track-bridge coupled braking system under earthquake. *Structures* **2023**, *53*, 1519–1529. [CrossRef]
26. Xiang, P.; Wei, M.; Sun, M.; Li, Q.; Jiang, L.; Liu, X.; Ren, J. Creep Effect on the Dynamic Response of Train-Track-Continuous Bridge System. *Int. J. Struct. Stab. Dyn.* **2021**, *21*, 2150139. [CrossRef]